DOI: 10.1002/ejic.200800482

A Strategy to Improve the Overall Performance of the Lithium Ion-Conducting Solid Electrolyte $Li_{0.36}La_{0.56}\square_{0.08}Ti_{0.97}Al_{0.03}O_3$

Yaoming Wang,[a] Zhanqiang Liu,[a] Fuqiang Huang,*[a] Jianhua Yang,[a] and Junkang Sun[a]

Keywords: Lithium ion conductivity / Solid electrolytes / Mechanical milling / Materials science / Amorphous materials

A strategy to improve the overall performance of the lithium ion-conducting solid electrolyte (Li-CSE) $Li_{0.36}La_{0.56}\square_{0.08}Ti_{0.97}Al_{0.03}O_3$ (LLTO) is proposed. Thin layers of the electronically insulating, electrochemically stable, and low-melting Li-CSE $Li_{3.25}Ge_{0.25}P_{0.75}S_4$ (LGPS) were coated onto LLTO powders, which resulted in oxide/sulfide composite electrolytes. The introduction of LGPS simultaneously brought about drastic reductions in the activation energies and great enhancements of the total ionic conductivities of the composite electrolytes. As the LGPS content was increased from 0 mol-% to 20 mol-%, the activation energy decreased steadily from 0.62 eV to 0.34 eV, and accordingly a total ionic conductivity as high as 1.62×10^{-4} S cm^{-1} was reached, almost the same as those of the excellent oxide-based Li-CSE ceramics sintered at extremely high temperatures, and a wide electrochemical window of over 6 V vs. Li^+/Li was achieved. In addition, a low electronic conductivity of 2.38×10^{-9} S cm^{-1} at room temperature for the composite electrolyte was discovered.

Introduction

Lithium ion-conducting solid electrolytes (Li-CSEs) have evoked great interest because of their intrinsic advantages over the traditional liquid electrolytes, such as thermal stability, absence of leakage and pollution, resistance to shocks and vibrations, large electrochemical windows of application, and facility of miniaturization.

The well studied Li-CSEs can be categorized into two classes: oxides and sulfides. A wide variety of oxide materials have been investigated as Li-CSEs, and some of them exhibit high bulk lithium ion conductivity; these include perovskite-type $Li_{3x}La_{(2/3)-x}\square_{(1/3)-2x}TiO_3$[1–7] and NASICON-structured $Li_{1+x}Ti_{2-x}M_x(PO_4)_3$ (M = Al, Ga, In, Sc),[8,9] with bulk conductivities of the magnitude of 10^{-3} S cm^{-1}. The also well studied[14–17] sulfide-based Li-CSEs are commonly superior to oxide-based Li-CSEs in their total ionic conductivity, due to the larger radius and greater polarizability of the sulfur anion in relation to the oxygen anion. A notably high total ionic conductivity of 2.2×10^{-3} S cm^{-1} at 25 °C, together with negligible electronic conductivity, high electrochemical stability, and no reaction with lithium metal, was achieved in the $Li_{3.25}Ge_{0.25}P_{0.75}S_4$ (LGPS) system,[15] much superior to any oxide-based Li-CSE. At the same time, however, sulfide-based Li-CSEs are generally easy to hydrolyze and hard to synthesize, whereas many ingredients utilized are environmentally malign; these factors are all unwanted for practical applications.

Oxide-based Li-CSEs, which are generally easy to synthesize, resistive to moisture, and environmentally benign, show great potential for practical applications in all solid-state lithium ion batteries. At present, the fastest oxide-based Li-CSE is the perovskite-type lithium lanthanum titanate, $Li_{0.36}La_{0.56}\square_{0.08}Ti_{0.97}Al_{0.03}O_3$ (LLTO), with its highest bulk conductivity of 2.95×10^{-3} S cm^{-1} at 295 K.[7] However, there are some significant obstacles to the actual utilization of LLTO as a Li-CSE: the poor ionic conduction of its grain boundary, leading to a low total ionic conductivity, chemical instability in direct contact with elemental lithium, a very narrow electrochemical window (about 1.7 V), and a significantly high electronic conductivity caused by the easy reduction of Ti^{4+} to Ti^{3+}.[10–13]

LLTO could readily be employed as a Li-CSE in all solid-state lithium ion batteries, provided that the drawbacks described above were conquered. Here we propose a strategy to improve the overall performance of the Li-CSE LLTO. A thin layer of the electronically insulating, electrochemically stable, and low-melting Li-CSE LGPS was coated onto LLTO powder to serve as a continuous grain boundary in LLTO, resulting in an oxide/sulfide composite electrolyte. The insulating thin LGPS layer can serve as an electronic shield to cut off the electronic conduction of the composite electrolyte. Therefore, the reduction/oxidation of Ti^{4+}/Ti^{3+} in LLTO can be prevented, owing to the fact that no (or nominal) electrons from the external circuit can be injected into the LLTO, resulting in a great enhancement of

[a] State Key Laboratory of High Performance Ceramics and Superfine Microstructures, Shanghai Institute of Ceramics, Chinese Academy of Sciences,
Shanghai 200050, P. R. China
Fax: +86-21-52413903
E-mail: huangfq@mail.sic.ac.cn

the electrochemical stability of the composite electrolytes. On the basis of that hypothesis, the electrochemical window of LLTO should be greatly broadened.

Results and Discussion

Figure 1 shows the X-ray diffraction (XRD) patterns of LLTO, 0.20 LGPS/0.80 LLTO, and LGPS, respectively. The as-prepared LLTO is a pure phase as characterized by XRD (JCPDS entry no. 87–0935 for standard pattern of LLTO). Almost no detectable peaks due to LGPS are present in the XRD pattern of the 0.20 LGPS/0.80 LLTO composite powder, which indicates that the LGPS powder was amorphorized by the high-energy ball milling, and no recrystallization occurred after heat treatment at 260 °C. The XRD pattern of poorly crystallized LGPS shown in Figure 1 is consistent with the reported data.[15]

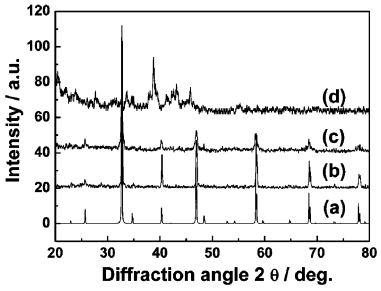

Figure 1. a) Standard powder X-ray diffraction pattern of LLTO from JCPDS entry no. 87–0935; b), c), d) powder X-ray diffraction patterns of the as-prepared LLTO powder, 0.20 LGPS/0.80 LLTO composite, and LGPS powder, respectively.

Figure 2 shows Nyquist plots of the composite electrolyte 0.20 LGPS/0.80 LLTO measured at different temperatures. The typical behavior of an impedance plot should consist of two parts: the semicircle, attributable to bulk and grain boundary contributions, in the high-frequency range and the spike, caused by the electrode contribution,[18,19] in the low-frequency range. The semicircles are usually present at frequencies lower than 0.1 MHz in Nyquist plots of LLTO ceramic samples at room temperature.[11] Here, though, there is no semicircle present in the plots within the measuring frequencies, even at the low temperature of 30 °C. It can thus be inferred that the ionic conductivity of the grain boundary of the composite electrolyte is highly enhanced.

The total conductivities of the samples of x LGPS/(1–x) LLTO (x = 0.00, 0.05, 0.10, 0.20, 1.00) were obtained from Nyquist plots at different temperatures. Figure 3 shows the reciprocal temperature dependence of the logarithmic conductivity for all the samples. With increasing LGPS content, increments of orders of magnitude in the total conductivities of the composite electrolytes were observed. It can be deduced that the ionic conductivity of the grain boundary of the composite electrolytes is highly enhanced, because the bulk conductivity of the composite electrolytes should remain unaffected. As the content of LGPS increased to 20 mol-%, total ionic conductivities of

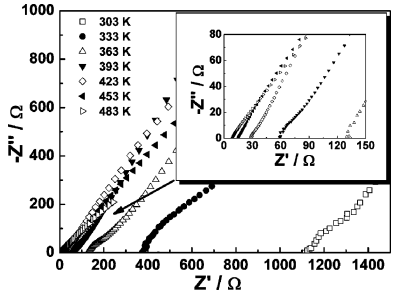

Figure 2. Impedance plots of the composite electrolyte 0.20 LGPS/0.80 LLTO.

the composite electrolytes as high as 1.62×10^{-4} S cm^{-1} were achieved, pretty much the same as that of the highest oxide-based Li-CSEs sintered at extremely high temperature.[20]

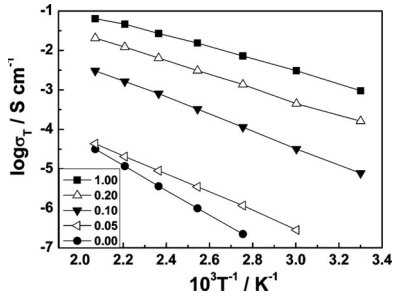

Figure 3. Reciprocal temperature dependence of the logarithmic conductivity for the samples of x LGPS/(1–x) LLTO (x = 0.00, 0.05, 0.10, 0.20, 1.00).

The activation energies (E_a) of the composite electrolytes were calculated over a temperature range of 30 °C to 210 °C by use of the following formula:

$$\sigma_T = \sigma_0 \exp(-\frac{E_a}{kT})$$

where σ_T is the total conductivity of the composite electrolyte at the definite temperature, σ_0 is the pre-exponential parameter, k is the Boltzmann constant, and T is the Kelvin temperature.

It can be calculated that the introduction of LGPS can effectively decrease the activation energies of the composite electrolytes even if the content of LGPS is very low (5 mol-%). This also accounts for the improvement in ionic conductivity of the grain boundary of the composite electrolytes. With increasing LGPS content up to 20 mol-%, the activation energies of the composite electrolytes decreased steadily from 0.62 eV to 0.34 eV.

The dc conductivity of the composite electrolyte 0.20 LGPS/0.80 LLTO was measured at room temperature. When lithium plates were used as nonblocking electrodes, the dc conductivity is almost constant with increasing time. The conductivity is around 4.4×10^{-5} S cm^{-1}, a little lower than the value (1.62×10^{-4} S cm^{-1} at 30 °C) obtained from the impedance measurement. This may be because that part of the applied potential was consumed at the interfaces between electrode and the electrolyte. When indium plates

were used as blocking electrodes to evaluate the electronic conductivity of the system at room temperature it was found that the conductivity was almost stabilized at around 2.38×10^{-9} S cm^{-1}, four orders of magnitude lower than the value obtained with use of lithium plates as nonblocking electrodes. Therefore the electronic conductivity of the sample can be neglected as compared with its ionic conductivity.[21]

The electrochemical stability of the composite electrolyte 0.20 LGPS/0.80 LLTO was examined by cyclic voltammetry of the Li/(0.20 LGPS/0.80 LLTO)/Pt cell with use of a lithium reference electrode and a scan rate of 1 mV s^{-1} as shown in Figure 4. Cathodic and anodic currents corresponding to lithium deposition ($Li^+ + e \rightarrow Li$) and dissolution ($Li \rightarrow Li^+ + e$), respectively, were observed. The result shows that there is no obviously anodic current due to sample decomposition observed in the potential up to 6.0 V vs. Li^+/Li, which is much higher than the 1.7 V value for pure LLTO.[11,22] This indicates that the proposed strategy had proved to be very effective. The insert figure shows the local magnification of the CV plot and illustrates that a very small oxidation peak of the electrolyte was observed at around 1.27 V, possibly resulting from the oxidation of Ti^{3+} to Ti^{4+}.[11,22] The reason for this may be that the LLTO was not perfectly coated by LGPS and that the coating process need to be further improved.

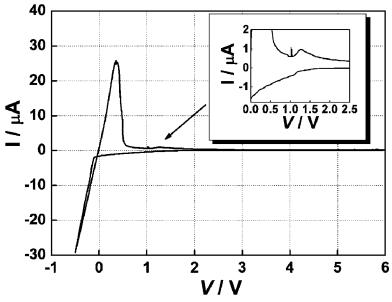

Figure 4. Cyclic voltammetry of the cell Li/(0.2 LGPS/0.8 LLTO)/Pt.

The FESEM image of the fracture surface of the composite electrolyte 0.20 LGPS/0.80 LLTO is shown in Figure 5. Apparently, there are two phases: the well crystallized LLTO prepared at the high temperature of 1200 °C and the poorly crystallized LGPS, present in the composite. LGPS was amorphorized by the high-energy ball milling and did not recrystallize during the following heat treatment at 260 °C as indicated by XRD. It can be observed that all grains of LLTO are isolated by the amorphous LGPS, which can not only improve the total ionic conductivities but also serve as the shields to cut off the electronic conduction of LLTO, resulting in a great enhancement of the electrochemical stability of the composite electrolyte.

Figure 6 shows a representation of the coating of LGPS on LLTO grains (i.e., the formation of a LGPS continuous grain boundary). The electronic insulation coating of LGPS can prevent the reduction/oxidation of LLTO at high potential, even far above the reduction/oxidation potential of Ti^{4+}/Ti^{3+}. A great enhancement of the electrochemical stability of the composite electrolyte and a wide electrochemical window of application can therefore be achieved, as has been established by the results shown in Figure 4. This may be the most attractive feature of the coating strategy proposed here. Such a strategy can be extended to the other systems: a wide-electrochemical-window composite electrolyte should be achievable as long as an insulating and electrochemical stable electrolyte is employed as the continuous grain boundary, regardless of whether the main ingredient of the composite may be chemical and/or electrochemical unstable, such as $Li_{1+x}Ti_{2-x}M_x(PO_4)_3$ (M = Al, Ga, In, Sc). The grain boundary may not only be the low-melting sulfide-based Li-CSEs but also low-melting oxide-based Li-CSEs such as Li_2O/B_2O_3, Li_2O/P_2O_5, and $Li_2O/B_2O_3/P_2O_5$ glass.[23–25]

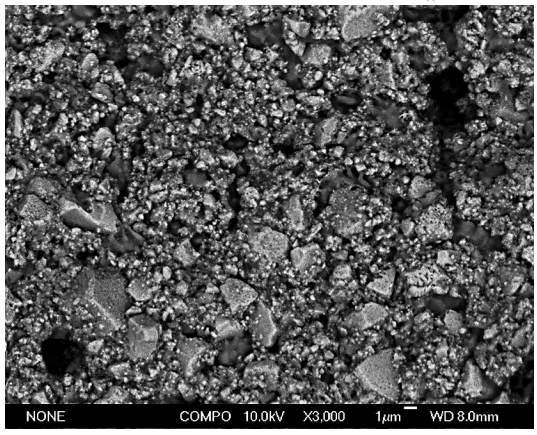

Figure 5. FESEM image of the fracture surface of the composite electrolyte 0.20 LGPS/0.80 LLTO.

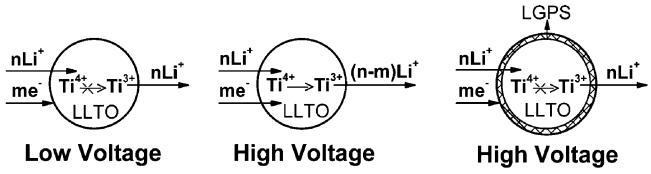

Figure 6. Simulated scheme of the coating of LGPS on LLTO.

Conclusions

A strategy to improve the overall performance of the lithium ion-conducting solid electrolyte $Li_{0.36}La_{0.56}\square_{0.08}Ti_{0.97}Al_{0.03}O_3$ has been proposed. A thin layer of the electronically insulating, electrochemically stable, and low-melting Li-CSE LGPS was coated on LLTO powder, resulting in oxide/sulfide composite electrolytes. The composite electrolytes were successfully prepared at extremely low temperature of 260 °C. The introduction of LGPS simultaneously brought about drastic reductions in the activation energies and great enhancements in the total ionic conductivities of the composite electrolytes. As the content of LGPS was increased from 0 mol-% to 20 mol-%, the activation energy

decreased steadily from 0.62 eV to 0.34 eV, and accordingly a total ionic conductivity as high as 1.62×10^{-4} S cm^{-1} was reached – almost the same as seen with the excellent oxide-based Li-CSE ceramics sintered at extremely high temperature – and a wide electrochemical window of over 6 V vs. Li^+/Li was achieved. In addition, a low electronic conductivity of 2.38×10^{-9} S cm^{-1} at room temperature for the composite electrolyte was discovered.

Experimental Section

Raw Materials Preparation: LLTO powder was synthesized from stoichiometric amounts of Li_2CO_3 (Sinopharm Chemical Reagent Co., Ltd., 4 N), La_2O_3 (Rare-chem. Hi-Tech Co., Ltd., >99.99%), TiO_2 (P25, Degussa), and Al_2O_3 (Sinopharm Chemical Reagent Co., Ltd., 99.99%). The mixture was finely ground and then heat-treated at 1000 °C for 12 h to decarbonation. Afterwards, the sample was subjected to high-energy ball milling for 4 h and was then pelleted and sintered at 1200 °C for 12 h. The obtained pellet was ground to provide the final LLTO powder. LGPS powder was prepared by sintering mixtures of the stoichiometric amounts of self-made Li_2S, GeS_2, and P_2S_5 at 700 °C for 8 h.

Samples Preparation: x LGPS/(1–x) LLTO (x = 0, 0.05, 0.10, 0.20 and 1.0) composite samples were prepared by high-energy ball milling (SPEX Certi*Prep* 8000 Mixer/Mill) of mixtures of LGPS and LLTO in different molar ratios for 2 h. Pellets of 10 mm diameter and about 1 mm thickness of the samples were prepared by first pressing the powder samples under a pressure of 100 MPa, and then firing them at 260 °C for 2 h. Indium plates were attached on both sides of the pellets to serve as current collectors.

Characterization: X-ray diffraction patterns were obtained (Rigaku D/Max-2550 V) with use of Cu-K_α radiation (λ = 0.15418 nm). The electrical behavior of all the samples of x LGPS/(1–x) LLTO was studied with the aid of an impedance analyzer (Chenhua 660B) in the temperature range of 30 °C to 210 °C at frequencies ranging from 0.1 Hz to 0.1 MHz under dry Ar. DC conductivity measurements were conducted for 0.20 LGPS/0.80 LLTO in a dry Ar flow at room temperature. Lithium plates were used as nonblocking electrodes and indium plates as blocking electrodes, respectively, to determine the dominant mobile ions and the electronic conductivity of the system. A dc constant potential of 1 V was applied. Cyclic voltammetry was carried out for the cell Li/(0.20 LGPS/0.80 LLTO)/Pt to evaluate the electrochemical stability of the composite electrolyte at room temperature. The scanning rate was set at 1 mV s^{-1}. The microstructure of the composite electrolyte 0.20 LGPS/0.80 LLTO pellet was characterized by field emission scanning electronic microscopy (FESEM); the FESEM image was obtained with a JEOL JSM 6700F NT instrument with an accelerating potential of 10.0 kV.

Acknowledgments

The research was financially supported by the Science and Technology Commission of Shanghai (Grant No. 08JC1420200 and 0752nm016), the National 973 Program of China (Grant No. 2007CB936704 and 2009CB939903) and the National Science Foundation of China (Grant No. 204710687).

[1] A. G. Belous, G. N. Novitskaya, S. V. Polyanetskaya, Yu. I. Gornikov, *Izv. Akad. Nauk SSSR, Neorg. Mater.* **1987**, *23*, 470–472.
[2] Y. Inaguma, C. Liquan, M. Itoh, T. Nakamura, T. Uchida, H. Ikuta, M. Wakihara, *Solid State Commun.* **1993**, *86*, 689–693.
[3] H. Kawai, J. Kuwano, *J. Electrochem. Soc.* **1994**, *141*, L78–L79.
[4] Y. Inaguma, C. Liquan, M. Itoh, T. Nakamura, *Solid State Ionics* **1994**, *70–71*, 196–202.
[5] Y. Inaguma, M. Itoh, *Solid State Ionics* **1996**, *86–88*, 257–260.
[6] Y. Harada, Y. Hirakoso, H. Kawai, J. Kuwano, *Solid State Ionics* **1999**, *121*, 245–251.
[7] A. Morata-Orrantia, S. García-Martín, M. A. Alario-Franco, *Chem. Mater.* **2003**, *15*, 3991–3995.
[8] H. Aono, E. Sugimoto, Y. Sadaoka, N. Imanaka, G. Adachi, *J. Electrochem. Soc.* **1989**, *136*, 590–591.
[9] H. Aono, E. Sugimoto, Y. Sadaoka, N. Imanaka, G. Adachi, *J. Electrochem. Soc.* **1990**, *137*, 1023–1027.
[10] P. Birke, S. Scharner, R. A. Huggins, W. Weppner, *J. Electrochem. Soc.* **1997**, *144*, L167–L169.
[11] C. H. Chen, K. Amine, *Solid State Ionics* **2001**, *144*, 51–57.
[12] X. M. Wu, X. H. Li, Y. H. Zhang, M. F. Xu, Z. Q. He, *Mater. Lett.* **2004**, *58*, 1227–1230.
[13] X. X. Xu, Z. Y. Wen, X. L. Yang, J. C. Zhang, Z. H. Gu, *Solid State Ionics* **2006**, *177*, 2611–2615.
[14] F. Mizuno, A. Hayashi, K. Tadanaga, M. Tatsumisago, *Adv. Mater.* **2005**, *17*, 918–921.
[15] R. Kanno, M. Murayama, *J. Electrochem. Soc.* **2001**, *148*, A742-A746.
[16] Y. Kim, J. Saienga, S. W. Martin, *J. Phys. Chem. B* **2006**, *110*, 16318–16325.
[17] F. Mizuno, A. Hayashi, K. Tadanaga, M. Tatsumisago, *Solid State Ionics* **2006**, *177*, 2721–2725.
[18] J. T. S. Irvine, D. C. Sinclair, A. R. West, *Adv. Mater.* **1990**, *2*, 132–138.
[19] V. Thangadurai, R. A. Huggins, W. Weppner, *J. Power Sources* **2002**, *108*, 64–69.
[20] S. Stramare, W. Weppner, *Ionics* **1999**, *5*, 405–409.
[21] V. Thangadurai, W. Weppner, *Chem. Mater.* **2002**, *14*, 1136–1143.
[22] M. Klingler, W. F. Chu, W. Weppner, *Ionics* **1997**, *3*, 289–291.
[23] S. W. Martin, C. A. Angell, *J. Non-Cryst. Solids* **1986**, *83*, 185–207.
[24] G. Chiodelli, A. Magistris, *Solid State Ionics* **1986**, *18–19*, 356–361.
[25] M. J. G. Jak, F. G. B. Ooms, E. M. Kelder, W. L. Legerstee, J. Schoonman, A. Weisenburger, *J. Power Sources* **1999**, *80*, 83–89.

Received: May 14, 2008
Published Online: November 12, 2008

